Chapter 2
Experiment

In this chapter, we introduce the experiment of relativistic heavy ion collision. We introduce the facility and detectors used for data taking. We also introduce the kinematic variables measured for this analysis.

2.1 Relativistic Heavy Ion Collider

The Relativistic Heavy Ion Collider (RHIC) is one of the high energy heavy-ion colliders located at Brookhaven National Laboratory in Upton, New York on Long Island. By accelerating and colliding heavy ion and polarized proton beams, physicists study the matter created at extremely high temperature and density, which is the QCD matter with strongly interacting partons (quarks and gluons).

Protons and heavy ion nuclei are accelerated in two independent pipes to nearly the speed of light and may collide at four intersecting points where the pipes cross. So far, several particle species have been accelerated for collisions at different energies, including proton-on-proton (p+p), deuterium-on-gold (d+Au), copper-on-copper (Cu+Cu), gold-on-gold (Au+Au), copper-on-gold (Cu+Au) and uranium-on-uranium (U+U). For heavy ion collisions, the center of mass energy can reach 200 GeV per nucleon pair. For p+p collisions, it achieved 500 GeV in 2009.

As shown in Fig. 2.1, the RHIC accelerator ring is 3,834 m long in circumference, and there are four experiments on RHIC collision points. They are STAR (6 o'clock), PHENIX (8 o'clock), PHOBOS (10 o'clock) and BRAHMS (1 o'clock). PHOBOS and BRAHMS have completed their commissioning and been shut down after 2005 and 2006, while STAR and PHENIX are still running since 2000. This thesis is based on the data taken by STAR experiment of Au+Au and d+Au collisions at $\sqrt{s_{NN}} = 200$ GeV.

Q. Wang, *Charge Multiplicity Asymmetry Correlation Study Searching for Local Parity Violation at RHIC for STAR Collaboration*, Springer Theses,
DOI 10.1007/978-3-319-00756-4_2, © Springer International Publishing Switzerland 2013

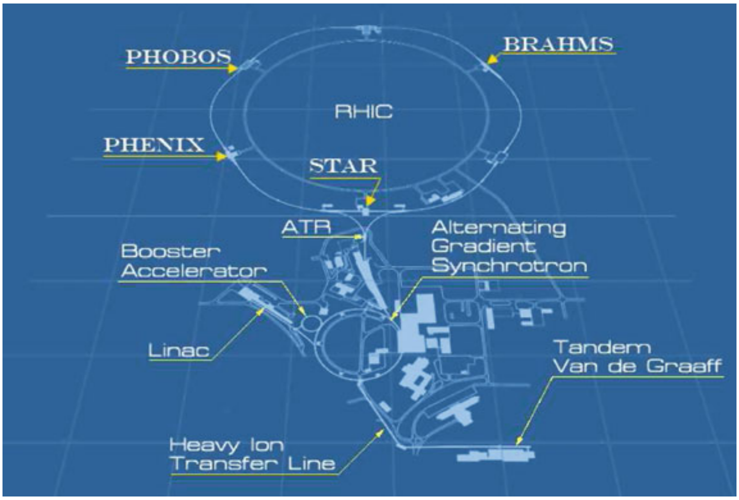

Fig. 2.1 The schematic plot of the Relativistic Heavy Ion Collider (RHIC) facility located at Brookhaven National Laboratory (BNL) (Diagram taken from [3])

2.2 STAR Experiment

The Solenoidal Tracker at RHIC (STAR) detector is located at the 6 o'clock interaction region of the RHIC accelerator ring. The main physics goal is to study the formation, evolution and characteristics of the strongly coupled Quark Gluon Plasma (sQGP) [5, 6, 9, 10], a state of QCD matter which is believed to be formed at very high temperature and/or high energy density. It is designed primarily for charged hadron production measurements with high precision tracking and momentum over a large solid angle.

STAR is a massive detector weighing 1,200 tons and as big as a building. It has a large relatively uniform acceptance in azimuthal angle, and also a large polar angle coverage in mid-rapidity. It consists of several sub-systems as shown in Fig. 2.2. System upgrades are constantly going on since the first build of the detector. Some of the sub-detectors are removed and replaced for better measurement or more tracking capability.

For convenience, we set up the STAR coordinate system with its origin located at the STAR detector geometry center. The z direction points to the west, which is parallel to the beam pipe direction. And the x direction points to the south, and the y direction points to up. The whole detector is surrounded by the main magnetic coil which generates a field in the z direction with the maximum of $|B_z| = 0.5\,\mathrm{T}$ [11].

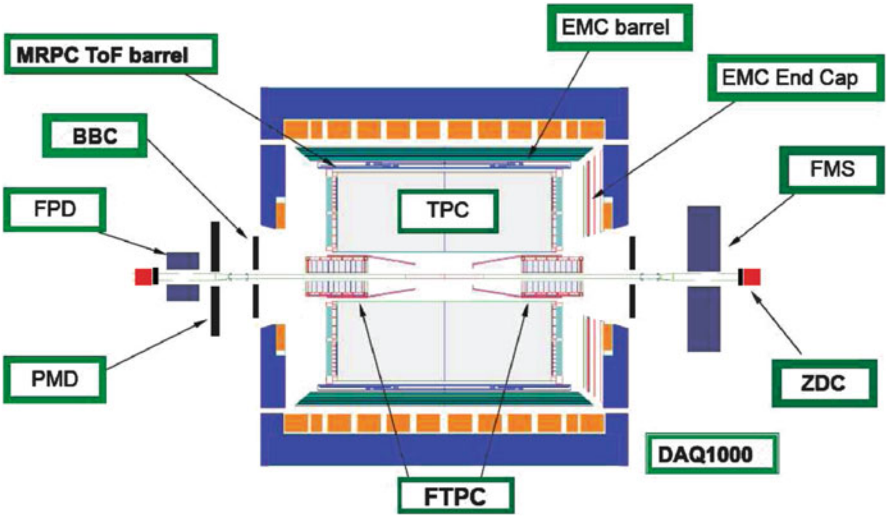

Fig. 2.2 Schematic STAR detector layout with selected sub-systems (Diagram taken from [3])

2.2.1 Time Projection Chamber

The main tracking device is the Time Projection Chamber (TPC), which records the tracks of particles and provides the kinematic information of each track [2, 8]. It is located within the magnetic coil, with a 4.2 m cylinder length, 0.5 m inner radii and 2 m outer radii. With the full magnetic field ($|B_z| = 0.5$ T) turned on, the TPC can identify a broad transverse momentum range of charged particles from 0.15 to 30 GeV/c depending on particles.

A diagram of the TPC is shown in Fig. 2.3. The TPC is a particle detector which consists of a gas-filled cylindrical chamber with multi-wire proportional chambers on the endcaps at each side of the cylinder. There is a high voltage central membrane disc which divides the cylindrical chamber into two halves. The central membrane, together with the "Outer Field Cage" and "Inner Field Cage" as shown in Fig. 2.3, provide a nearly uniform electric field along the z direction parallel to the beam pipe and magnetic field, pointing from the endcaps to the center.

When a charged particle is generated in the collision, it traverses the TPC volume, ionizes gas atoms every few tenths of a millimeter along its trajectory, and leaves a cluster of electrons behind. The electron clusters then drift within the electric field toward the sectors of the endcaps. Each electron cluster will be accelerated by the electric field around the anode and cause a localized cascade of ionization, which is collected on the high voltage wire and results in an electric current. The position of the hit point is then recorded in the r and ϕ dimension, and the amplitude of the current is proportional to the energy of the detected particle. The endcaps are made by 24 identical sectors, 12 on each side. Each sector covers about $\pi/6$ in azimuthal

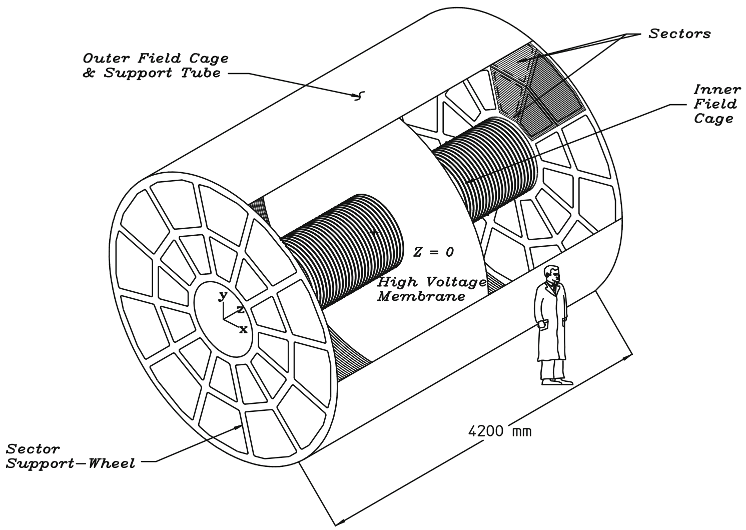

Fig. 2.3 The schematic cutaway view of STAR TPC detector (Figure is taken from [8])

angle, and totally full coverage of 2π. The z position is obtained by measuring the drift time from the collision to the time when the electron cluster is recorded at the endcaps because the drift velocity can be precisely measured beforehand. One can then reconstruct the tracks by fitting the 3-dimensional hit points collected by the TPC. Track in the TPC usually has a helix shape, and the maximum hit points at the endcaps can be as many as 45 hits. The transverse momentum p_T and the charge sign of a particle can be calculated from the curvature of the trajectory with the applied magnetic field. Figure 2.4 shows the side view (xz plane), and front view (xy plane) of an Au+Au collision event.

In this thesis, the particle information is taken mostly from the TPC. The most frequently used kinematic variables ϕ and η are shown in Fig. 2.4. The azimuthal angle ϕ (Fig. 2.4a) is the angle of a particle transverse momentum p_T relative to x axis in STAR coordinates. Pseudo-rapidity η describes the angle relative to the beam direction, i.e. z direction. It is defined as

$$\eta = -\ln\left[\tan\left(\frac{\theta}{2}\right)\right] \tag{2.1}$$

$$= \frac{1}{2}\ln\left(\frac{|\vec{p}|+p_L}{|\vec{p}|-p_L}\right), \tag{2.2}$$

where θ is the angle of the particle momentum $\vec{p}$ relative to the beam axis, and p_L denotes the longitudinal component of the particle momentum $\vec{p}$. In the relativistic limit when particle's speed is close to the speed of light, or the particle mass is small compared to its total energy, the rest mass could be ignored to good approximation. Then pseudo-rapidity is numerically close to rapidity which is defined as

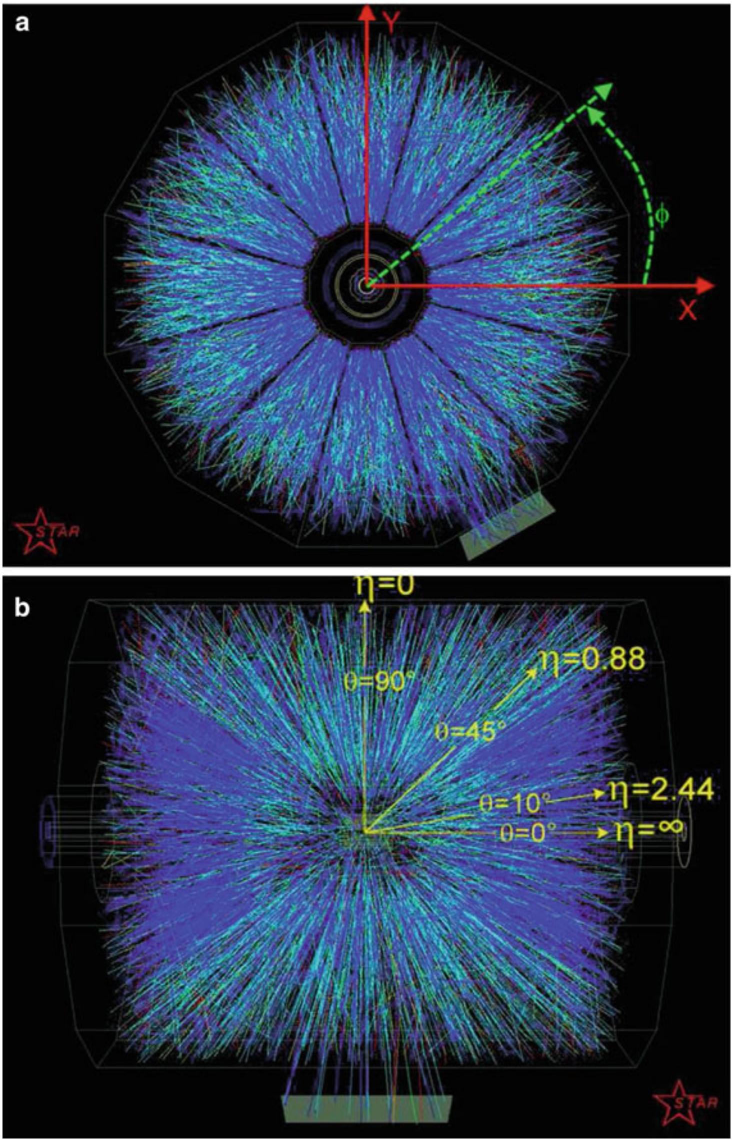

Fig. 2.4 An example event of central Au+Au collisions in transverse view (**a**) and side view (**b**). The definition of azimuthal angle ϕ and pseudo-rapidity η are shown in panel (**a**) and (**b**) respectively

$$y = \frac{1}{2} \ln \left(\frac{E + p_L}{E - p_L} \right), \tag{2.3}$$

where E is the energy of the particle. The rapidity definition is used in theoretical calculations, while it requires two parameters E and $\vec{p}$ of a particle to be measured at the same time, which is inconvenient experimentally. However, the pseudo-rapidity requires only one measurement, $\vec{p}$, and it is close to rapidity for light particles (i.e. pions, electrons). The STAR detector has a large and uniform pseudo-rapidity coverage of $-1 < \eta < 1$.

When an event is recorded, the tracks reconstructed from the TPC hits are called global tracks. By extrapolating the tracks back to the center of the detector, the original collision vertex can then be fitted from all the trajectories very precisely. The position of the collision vertex is noted as $\vec{v}$ in STAR coordinates. We can then do the tracking reconstruction again with all the TPC hits plus the additional collision vertex. The tracks reconstructed with collision vertex are called primary tracks. The advantage of primary tracks is that particles created from the collision vertex will get a better resolution since the collision vertex has a very good resolution. However, the tracks from secondary decay will have worse resolution because the collision vertex might be off from the track helix. Thus, we introduce the Distance of Closest Approach (DCA). It is defined as the closest distance from the collision vertex to a track helix. By cutting on DCA, one can manually select the tracks preferentially from the collision vertex or the secondary decay vertex.

2.2.2 Zero Degree Calorimeters

The Zero Degree Calorimeter (ZDC) detectors are located at ± 18 m away from the geometry center of the STAR detector as shown in red in Fig. 2.2 [7]. They measure the energy deposition of neutrons, which are associated with the spectator matter, in the three tungsten plates on each side of the ZDC. The ZDC has been used for beam monitoring and event triggering.

There was an upgrade in 2003 of the ZDC by adding Shower Maximum Detectors (SMD), which gives the ZDC-SMD the capability of recording the shower profile of neutron clusters in the transverse plane (xy plane) of the collisions. The SMD information contains 7-slate (vertical) by 8-slate (horizontal) readouts from the ADC photomultiplier tubes which connect to the SMD scintillators. The raw readouts are corrected for the background by subtracting the pedestal. The readouts also have to be adjusted for the distortion of the electronics by applying the gain correction, which is from the cosmic ray calibration. Finally, the vertical and horizontal signals can present a well defined spectator position in the xy plane, which can be used for the direct event-plane reconstruction.

2.2.3 Event Triggering

The collision rate at RHIC 2004 is about 10M Hz, which means there are 10M collision events per second happening in the STAR detector. However, the STAR TPC is a slow detector because the electrons need time to drift to the endcaps to be recorded, and the DAQ system is also limited by the bandwidth. At 2004, the DAQ operated at rates about 100 Hz of Au+Au 200 GeV collisions.

In order to reduce the recorded collision events, trigger detectors are needed to select 100 events out of 10M events per second, based on our interests [12]. The fast detectors are used as trigger detectors. They are the Zero Degree Calorimeters (ZDC), the Central Trigger Barrel (CTB) and the Beam-Beam Counters (BBC). The ZDC is introduced in previous section. The CTB detector is located between the outer cage of the TPC and the ToF detector, which measures the charge multiplicity in the same pseudo-rapidity range of $|\eta| < 1$ as the TPC with full azimuthal coverage. The BBC detector is located outside of the pole tip magnets as shown in Fig. 2.2. It measures the multiplicity in forward region and provides vertex location information of the collision.

The Au+Au minimum bias collisions, the least biased data sample, are triggered by both ZDCs (east- and west-side) and the CTB. The event is cut on the ZDC coincidence rate above certain value from the east and west ZDC, and the primary vertex from the ZDC signals. And there is also a cut on the CTB multiplicity to reject the non-hadronic events. However, some of the low multiplicity hadronic events are also rejected, thus there are bias on the low multiplicity events at the most peripheral collisions below 80 % centrality. For this reason, our analysis is focusing on the data above 80 % centrality only.

The d+Au minimum bias collisions used in this analysis are triggered on ZDC detector from the east side only, which is where the Au beam is from.

We also use the most central Au+Au collisions in the analysis which are triggered on ZDC detectors and the CTBs. It requires the ZDC detector with a high coincidence rate, and the CTBs with a large multiplicity matching the most central minimum bias collisions, which eventually selects the most central collisions about 12 % centrality.

2.2.4 Centrality Definition

The collision initial condition is of great importance in heavy ion nucleus-nucleus collisions. The impact parameter b is defined as the distance between the geometric center of the two colliding nuclei in the transverse plane. The nucleons are then undergo interactions with each other. The number of participants referred to as N_{part} is defined as the number of nucleons that participate in at least one inelastic nucleon-nucleon reactions. And the number of binary collisions is defined as the number of such inelastic nucleon-nucleon reactions, usually referred to as N_{coll}. However,

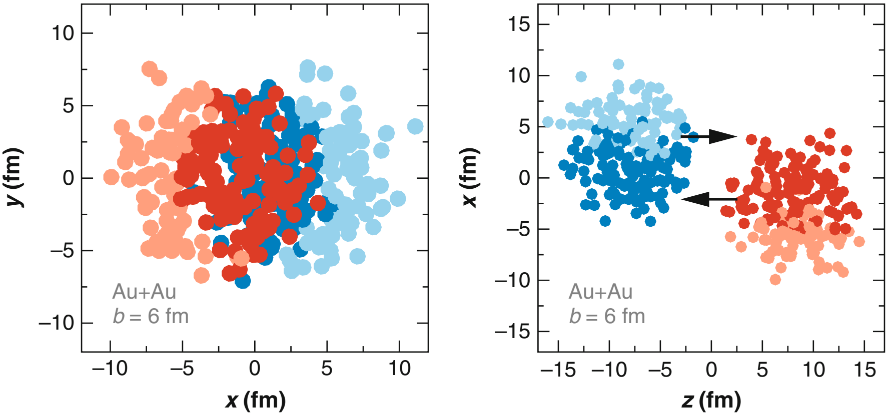

Fig. 2.5 A Glauber Monte-Carlo event (Au+Au at $\sqrt{s_{NN}} = 200$ GeV with impact parameter $b = 6$ fm) viewed in transverse plane (*left*) and along the beam axis (*right*) (Figure is taken from [13])

they cannot be measured directly from the experiment, and have to be deduced from other experimental observables and combined with Monte-Carlo simulations. The simulation is done in the geometry model with experimental measurement of nucleon-nucleon cross sections and considering the multiple scattering of nucleons in the heavy ion collisions. Such Monte-Carlo techniques is generally referred to as Glauber model [13].

Figure 2.5 shows a Glauber Monti-Carlo Au+Au collision event at center of mass $\sqrt{s_{NN}} = 200$ GeV. The impact parameter $b = 6$ fm. The dark circles represent the participating nucleons. It is obvious that the smaller the impact parameter, the more participating nucleons and binary collisions in an event, hence more generated particles detected by the detector. Figure 2.6 shows the illustration plot of the event multiplicity within $|\eta| < 1$ distribution corresponding to the impact parameter b and the number of participants N_{part}. Then experimentally, one can relate the final state multiplicity to the N_{part} and b.

In the STAR experiment, the efficiency uncorrected charged particle multiplicity in one unit of the pseudo-rapidity $dN_{ch}/d\eta$ is used instead of N_{ch} to deduce the N_{part} and b parameters, which is called reference multiplicity $N_{RefMult}$ [1,4]. The $N_{RefMult}$ is the number of charged particles recorded by the main TPC at mid-rapidity range of $-0.5 < \eta < 0.5$. With the $N_{RefMult}$ distribution, we can cut on certain fraction of the events to correspond to the impact parameter b and N_{part}. Typically, we cut on 0–5 %, 5–10 %, 10–20 %, 20–30 %, 30–40 %, 40–50 %, 50–60 %, 60–70 % and 70–80 % from most central to most peripheral collisions.

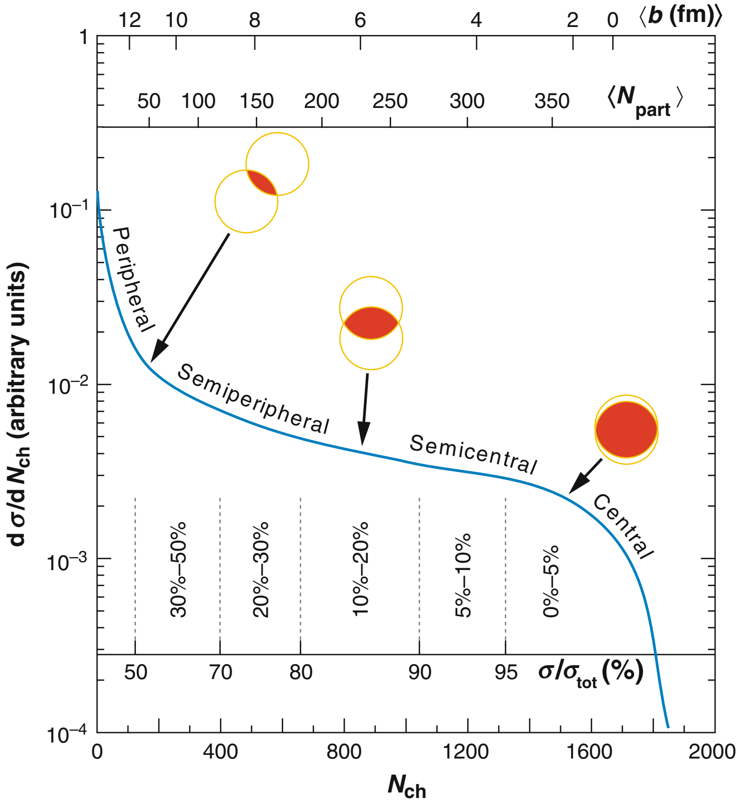

Fig. 2.6 An illustrated example of the total final state inclusive charged particle multiplicity N_{ch} distribution with Glauber-calculated quantities (b, N_{part}). The plotted distribution and various values are illustrative and not actual measurements (Figure is taken from [13])

References

1. Abelev, B., et al.: Systematic measurements of identified particle spectra in *pp*, d+Au and Au+Au collisions from STAR. Phys. Rev. **C79**, 034909 (2009). doi:10.1103/PhysRevC.79.034909
2. Ackermann, K., et al.: The STAR time projection chamber. Nucl. Phys. **A661**, 681–685 (1999). doi:10.1016/S0375-9474(99)85117-3
3. Ackermann, K., et al.: STAR detector overview. Nucl. Instrum. Methods **A499**, 624–632 (2003). doi:10.1016/S0168-9002(02)01960-5
4. Adams, J., et al.: Identified particle distributions in pp and Au+Au collisions at $\sqrt{s_{NN}} =$ 200 GeV. Phys. Rev. Lett. **92**, 112301 (2004). doi:10.1103/PhysRevLett.92.112301
5. Adams, J., et al.: Experimental and theoretical challenges in the search for the quark gluon plasma: the STAR collaboration's critical assessment of the evidence from RHIC collisions. Nucl. Phys. **A757**, 102–183 (2005). doi:10.1016/j.nuclphysa.2005.03.085

6. Adcox, K., et al.: Formation of dense partonic matter in relativistic nucleus nucleus collisions at RHIC: experimental evaluation by the PHENIX collaboration. Nucl. Phys. **A757**, 184–283 (2005). doi:10.1016/j.nuclphysa.2005.03.086
7. Adler, C., Denisov, A., Garcia, E., Murray, M., Strobele, H., et al.: The RHIC zero-degree calorimeters. Nucl. Instrum. Methods **A499**, 433–436 (2003). doi:10.1016/j.nima.2003.08.112
8. Anderson, M., Berkovitz, J., Betts, W., Bossingham, R., Bieser, F., et al.: The STAR time projection chamber: a unique tool for studying high multiplicity events at RHIC. Nucl. Instrum. Methods **A499**, 659–678 (2003). doi:10.1016/S0168-9002(02)01964-2
9. Arsene, I., et al.: Quark gluon plasma and color glass condensate at RHIC? The perspective from the BRAHMS experiment. Nucl. Phys. **A757**, 1–27 (2005). doi:10.1016/j.nuclphysa.2005.02.130
10. Back, B., et al.: The PHOBOS perspective on discoveries at RHIC. Nucl. Phys. **A757**, 28–101 (2005). doi:10.1016/j.nuclphysa.2005.03.084
11. Bergsma, F., et al.: The STAR detector magnet subsystem. Nucl. Instrum. Methods **A499**, 633–639 (2003). doi:10.1016/S0168-9002(02)01961-7
12. Bieser, F., Crawford, H., Engelage, J., Eppley, G., Greiner, L., et al.: The STAR trigger. Nucl. Instrum. Methods **A499**, 766–777 (2003). doi:10.1016/S0168-9002(02)01974-5
13. Miller, M.L., Reygers, K., Sanders, S.J., Steinberg, P.: Glauber modeling in high energy nuclear collisions. Annu. Rev. Nucl. Part. Sci. **57**, 205–243 (2007). doi:10.1146/annurev.nucl.57.090506.123020

Springer

http://www.springer.com/978-3-319-00755-7

Charge Multiplicity Asymmetry Correlation Study Searching for Local Parity Violation at RHIC for STAR Collaboration

Wang, Q.

2013, XXI, 134 p. 77 illus., 72 illus. in color., Hardcover
ISBN: 978-3-319-00755-7